

# A novel benzo[1,2-b:4,5-b']dithiophene-based conjugated polymer with a pendant diketopyrrolopyrrole unit for high-performance solar cells

Hua Tan,<sup>†</sup> Xianping Deng,<sup>†</sup> Junting Yu,<sup>†</sup> Baofeng Zhao,<sup>‡</sup> Yafei Wang,<sup>†</sup> Yu Liu,<sup>†</sup> Weiguo Zhu,<sup>\*,†</sup> Hongbin Wu,<sup>\*,‡</sup> and Yong Cao<sup>‡</sup>

<sup>†</sup>*Key Lab of Environment-Friendly Chemistry and Application of the Ministry of Education, College of Chemistry, Xiangtan University, Xiangtan 411105, China*

<sup>‡</sup>*Institute of Polymer Optoelectronic Materials and Devices, State Key Laboratory of Luminescent Materials and Devices, South China University of Technology, Guangzhou 510640, China*

## Content

1. General considerations for characterization
2. Device fabrication and characterization
3. The GPC elution curve of PBDT-TDPP-S
4. TGA measurement
5. Cyclic voltammetry curve measurement
6. Photovoltaic Properties of the PBDT-TDPP-S-based PSCs at different conditions
7. Electron mobility measurement (SCLC)
8. Impact of thermal annealing on film morphologies
9. <sup>1</sup>H NMR data for compound 2, M2, PBDT-TDPP-S, MS data for M2 and the infrared spectrum of PBDT-TDPP-S

## 1. General considerations for characterization

**Measurements:** Nuclear magnetic resonance (NMR) spectra were recorded on a Bruker DRX 400 spectrometer using tetramethylsilane as a reference in deuterated chloroform solution at 298 K. MALDI-TOF mass spectrometric measurements were performed on Bruker Biflex III MALDI-TOF. Molecular weight was determined using a Waters GPC 2410 in THF via a calibration curve of polystyrene as standard. Thermogravimetric analysis (TGA) was conducted under a dry nitrogen gas flow at a heating rate of  $20\text{ }^{\circ}\text{C min}^{-1}$  on a Perkin-Elmer TGA 7. The FT-IR spectra were recorded on a Perkin-Elmer Spectrum One Fourier transform infrared spectrometer by incorporating samples in KBr discs. UV-Vis absorption spectra were recorded on a HP-8453 UV visible system. Cyclic voltammetry was carried out on a CHI660A electrochemical work station in a three-electrode cell dipped in a 0.1M tetrabutyl-ammonium hexafluorophosphate ( $\text{Bu}_4\text{NPF}_6$ ) acetonitrile solution under nitrogen protection at a scan rate of 100 mV/s and room temperature (RT). In this three-electrode cell, a platinum rod, platinum wire and saturated calomel electrode were used as a working electrode, counter electrode and reference electrode, respectively. The morphology of the polymer/PCBM blend film was investigated by an atomic force microscopy (AFM) on a Veeco, DI Multimode NS-3D apparatus in a trapping mode under normal air condition at RT.

## 2. Device fabrication and characterization

**Device Fabrication:** Polymer solar cells were fabricated using indium tin oxide (ITO) glass as an anode, LiF/Al as a cathode, and a blend film of the polymer and PCBM as a photosensitive layer. After a 30 nm buffer layer of poly-(3,4-ethylenedioxythiophene) and polystyrene sulfonic acid (PEDOT:PSS) was spin-coated onto the precleaned ITO substrate, the photosensitive layer was subsequently prepared by spin-coating a solution of the polymer and PCBM (1:1.3, w/w) in chlorobenzene on the PEDOT:PSS layer with a typical concentration of  $20\text{ mg mL}^{-1}$ , followed by annealing at  $120\text{ }^{\circ}\text{C}$  for 10 minutes to remove chlorobenzene. LiF (0.7 nm) and Al (100 nm) were successively deposited on the photosensitive

layer in vacuum and used as top electrodes. The current–voltage ( $I$ – $V$ ) characterization of the devices was carried out on a computer-controlled Keithley 236 source measurement system. A solar simulator was used as the light source and the light intensity was monitored by a standard Si solar cell. The active area was  $7 \times 10^{-2}$  cm<sup>2</sup> for each cell. The thicknesses of the spun-cast films were recorded by a profilometer (Alpha-Step 200, Tencor Instruments). The incident photon-to-current conversion efficiency (IPCE) spectrum was measured by a Stanford research systems model SR830 DSP lock-in amplifier coupled with WDG3 monochromator and a 500 W xenon lamp.

Hole mobility of the PBDT-TDPP-S/PC<sub>71</sub>BM(w:w, 1:1.3) blend film was measured according to a similar method described in the literature<sup>[1-2]</sup>, using a diode configuration of ITO/PEDOT:PSS(40nm)/active layer/ MoO<sub>3</sub>/Al(100 nm) by taking current-voltage current in the range of 0-4 V and fitting the results to a space charge limited form, where the space charge limited current (SCLC) is described by  $J = 9\epsilon_0\epsilon_r\mu_h V^2/8L^3$ , where  $J$  is the current density,  $L$  is the film thickness of active layer,  $\mu_h$  is the hole mobility,  $\epsilon_r$  is the relative dielectric constant of the transport medium,  $\epsilon_0$  is the permittivity of free space ( $8.85 \times 10^{-12}$  F m<sup>-1</sup>),  $V$  is the internal voltage in the device and  $V = V_{\text{appl}} - V_a - V_{\text{bi}}$ , where  $V_{\text{appl}}$  is the applied voltage to the device,  $V_a$  is the voltage drop due to contact resistance and series resistance across the electrodes, and  $V_{\text{bi}}$  is the built-in voltage due to the relative work function difference of the two electrodes.

Electron mobility measurements of the PBDT-TDPP-S/PC<sub>71</sub>BM(w:w, 1:1.3) blend film were done using a similar method described in the literature with the following diode structures: ITO/Al(30 nm)/active layer/Ca(5nm)/Al(100 nm).<sup>[1-2]</sup> The charge carrier mobilities were calculated using the space-charge limited current (SCLC) model as describe above.

### 3. The GPC elution curve of PBDT-TDPP-S

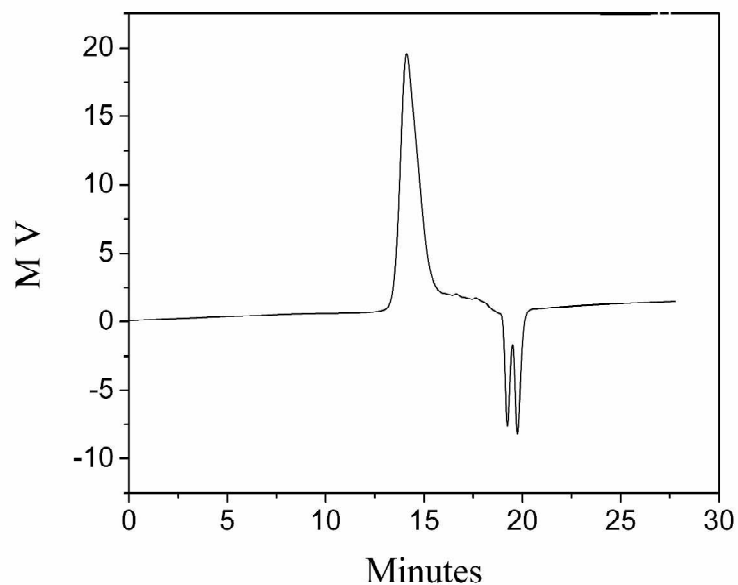


**Figure S1.** The GPC elution curve of PBDT-TDPP-S

### 4. TGA measurement

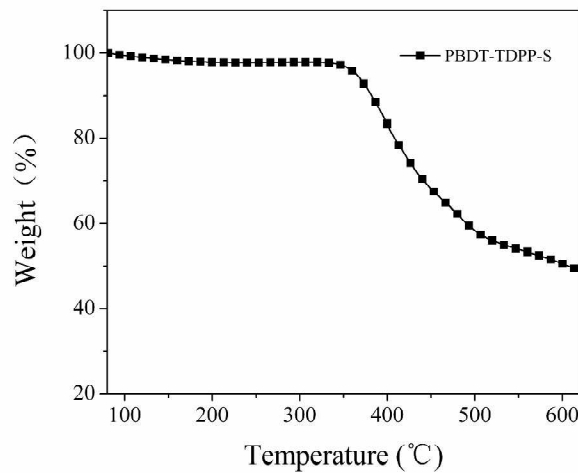


**Figure S2.** TGA curve of PBDT-TDPP-S at a scan rate of 20 °C/min under nitrogen atmosphere

## 5. Cyclic voltammetry curve measurement

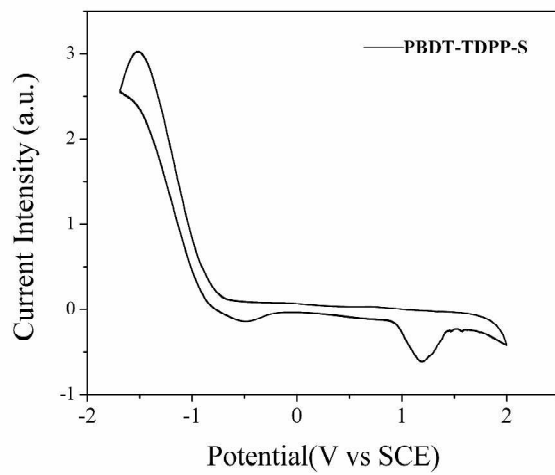


**Figure S3.** Electrochemical cyclic voltammetry curve of PBDT-TDPP-S

## 6. Photovoltaic Properties of the PBDT-TDPP-S-based PSCs at different conditions

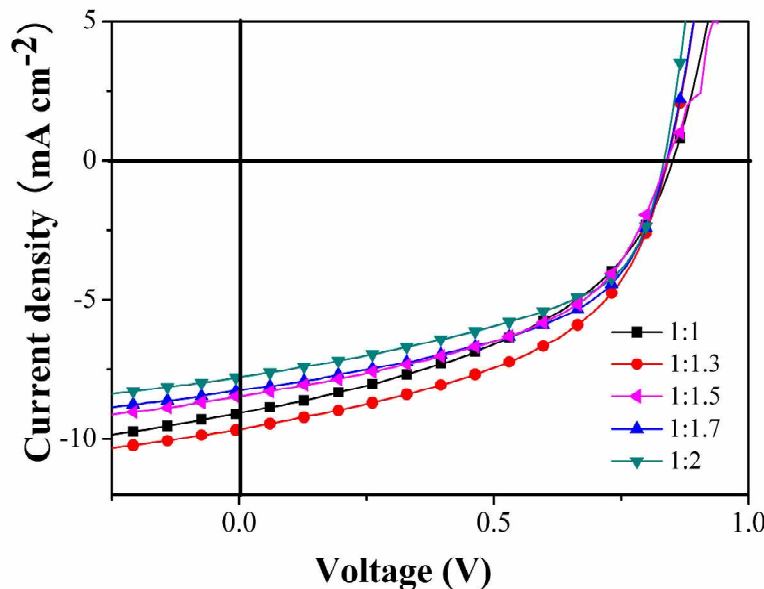


**Figure S4.**  $J$ - $V$  curves of the PBDT-TDPP-S:PC<sub>71</sub>BM PSCs with different blend ratios (w/w) at thickness of 80 nm and thermal annealing temperature of 90°C

**Table S1.** Photovoltaic properties of the PBDT-TDPP-S:PC<sub>71</sub>BM PSCs with different blend ratios (w/w) at thickness of 80 nm and thermal annealing temperature of 90°C

D/A Ratio	$J_{sc}$ / mA cm <sup>-2</sup>	$V_{oc}$ / V	FF / %	PCE <sub>max</sub> / %
1:1	9.07	0.85	45	3.58
1:1.3	9.65	0.84	49	4.15
1:1.5	8.26	0.84	51	3.70
1:1.7	7.77	0.83	51	3.41
1:2	7.45	0.84	49	3.19

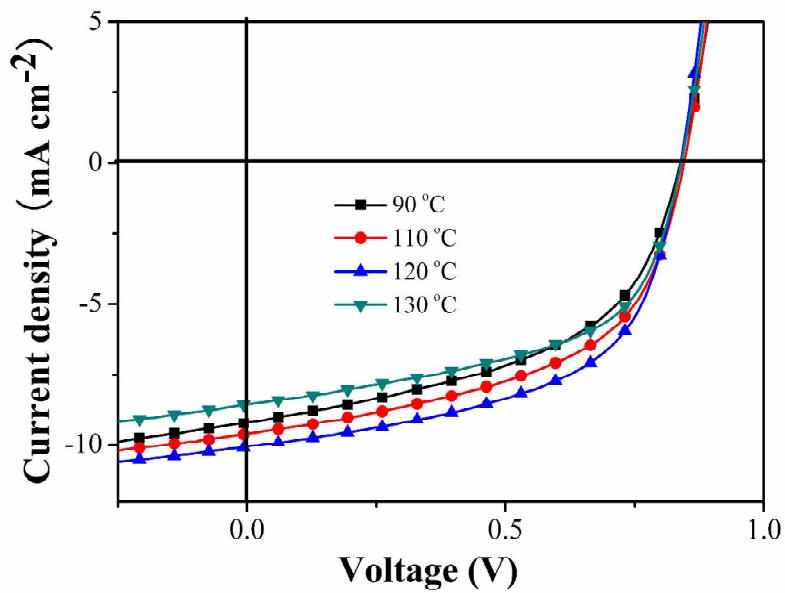


**Figure S5.**  $J$ - $V$  curves of the PBDT-TDPP-S:PC<sub>71</sub>BM PSCs with a thickness of 80 nm and a PBDT-TDPP-S/PC<sub>71</sub>BM ratio of 1:1.3 at different pre-thermal annealing temperatures.

**Table S2.** Photovoltaic properties of the PBDT-TDPP-S:PC<sub>71</sub>BM PSCs with a thickness of 80 nm and a PBDT-TDPP-S/PC<sub>71</sub>BM ratio of 1:1.3 at different pre-thermal annealing temperatures

Temperatures (°C)	$J_{sc}$ / mA cm <sup>-2</sup>	$V_{oc}$ / V	FF / %	PCE <sub>max</sub> / %
90	9.20	0.84	50	4.04
110	9.59	0.84	53	4.47
120	10.04	0.84	56	4.89
130	8.56	0.84	55	4.10

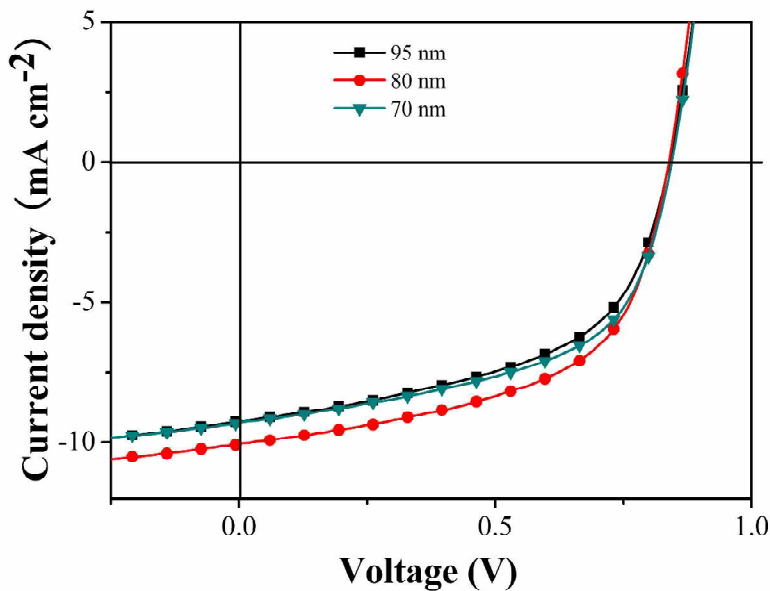
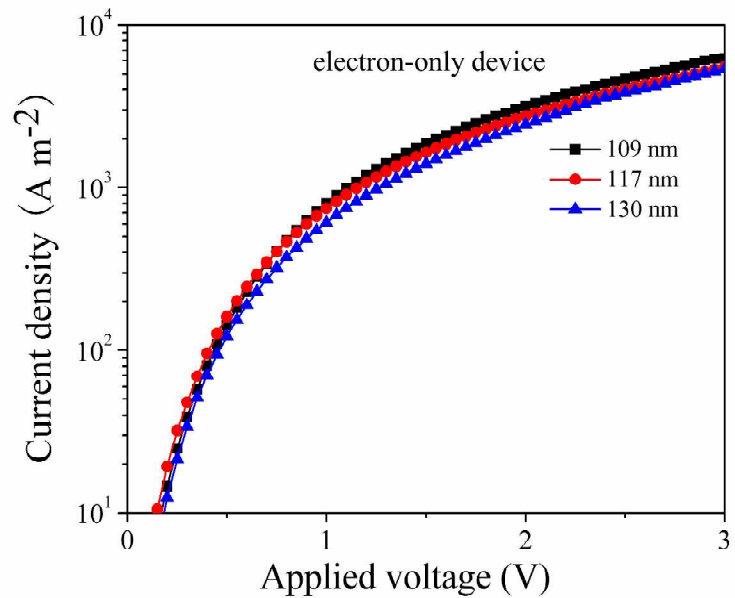


**Figure S6.**  $J$ - $V$  curves of the PBDT-TDPP-S: PC<sub>71</sub>BM PSCs with a PBDT-TDPP-S/PC<sub>71</sub>BM ratio of 1:1.3 under pre-thermal annealing temperature of 120 °C at different thicknesses

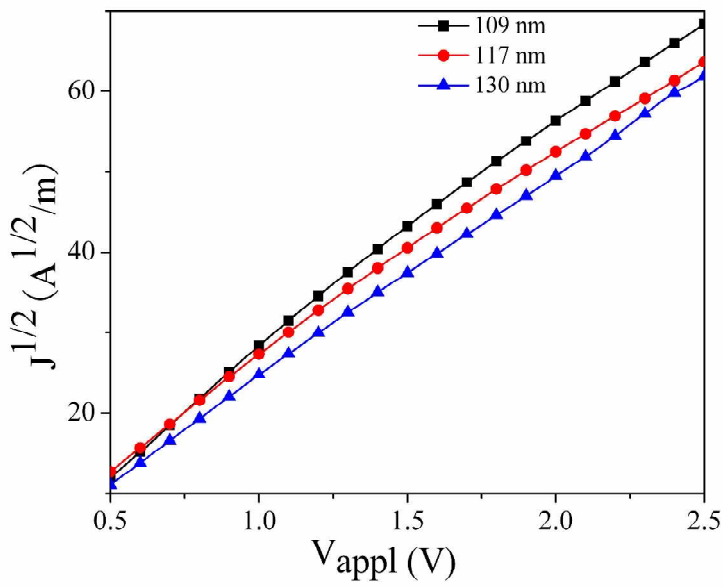
**Table S3.** Photovoltaic properties of the PBDT-TDPP-S: PC<sub>71</sub>BM PSCs with a PBDT-TDPP-S/PC<sub>71</sub>BM ratio of 1:1.3 under pre-thermal annealing temperature of 120 °C at different thicknesses

Donor	Acceptor	Thickness / nm	$J_{sc}$ / mA cm <sup>-2</sup>	$V_{oc}$ / V	FF / %	PCE <sub>max</sub> / %
PBDT-TDPP-S	PC <sub>71</sub> BM	95	9.25	0.84	53	4.31
PBDT-TDPP-S	PC <sub>71</sub> BM	80	10.04	0.84	56	4.89
PBDT-TDPP-S	PC <sub>71</sub> BM	70	9.30	0.84	55	4.51

## 7. Electron mobility measurements (SCLC)



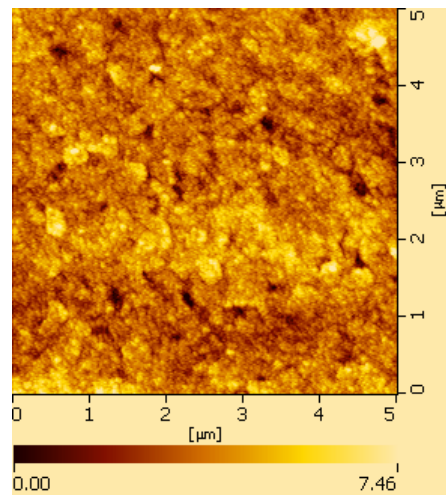
(a)



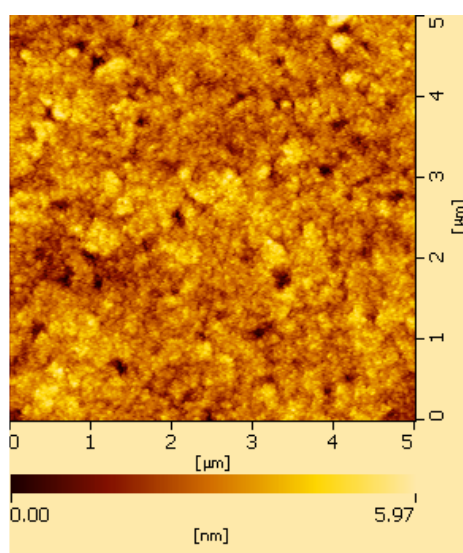
(b)

**Figure S7.** (a)  $J$ - $V$  characteristics, (b)  $J^{1/2}$ - $V$  characteristics of PBDT-TDPP-S electron-only devices with different thicknesses measured at ambient temperature

## 8. Impact of thermal annealing on film morphologies



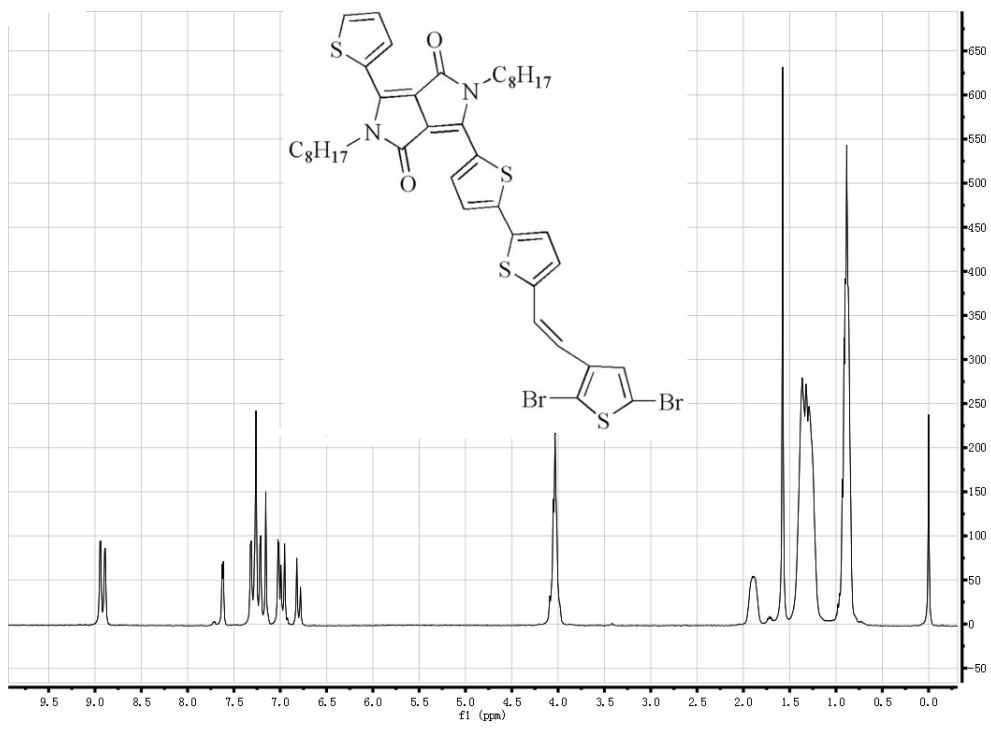
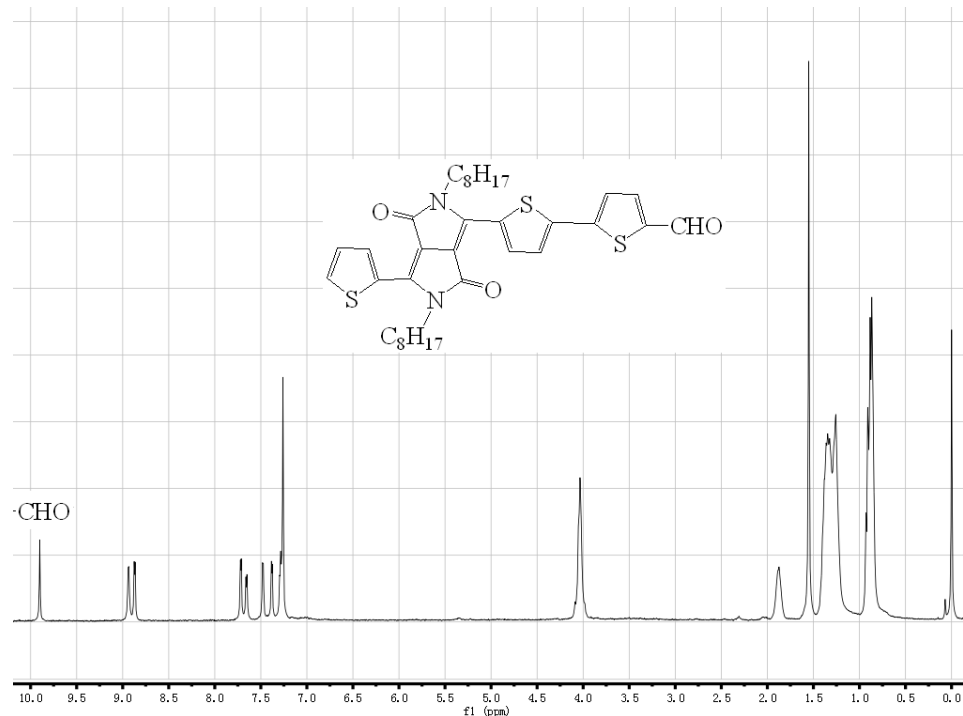
(a)

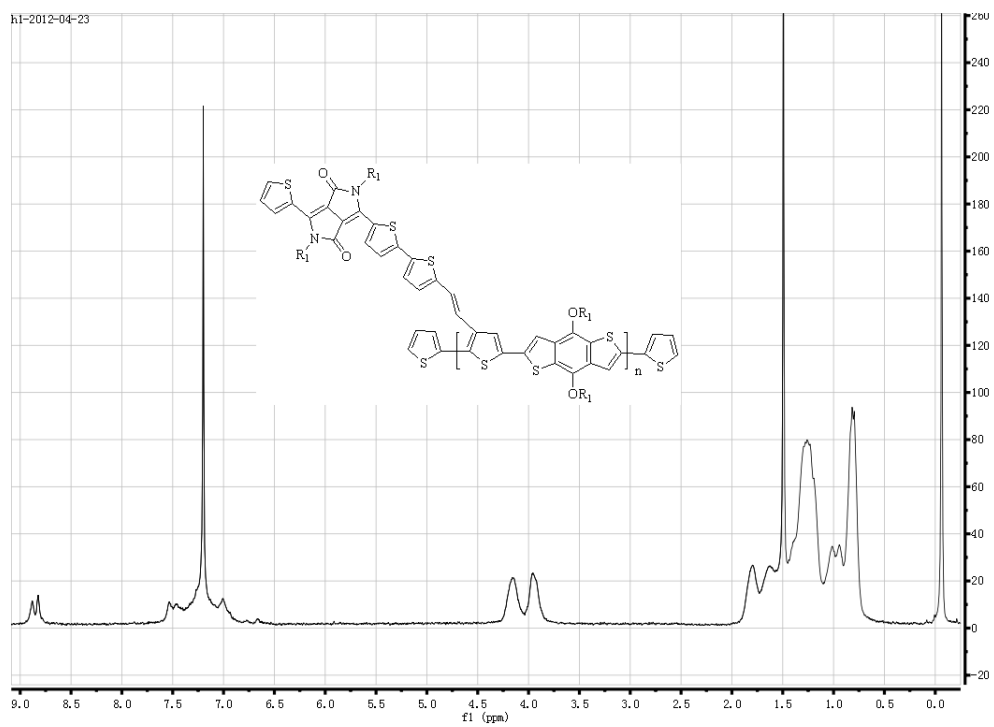
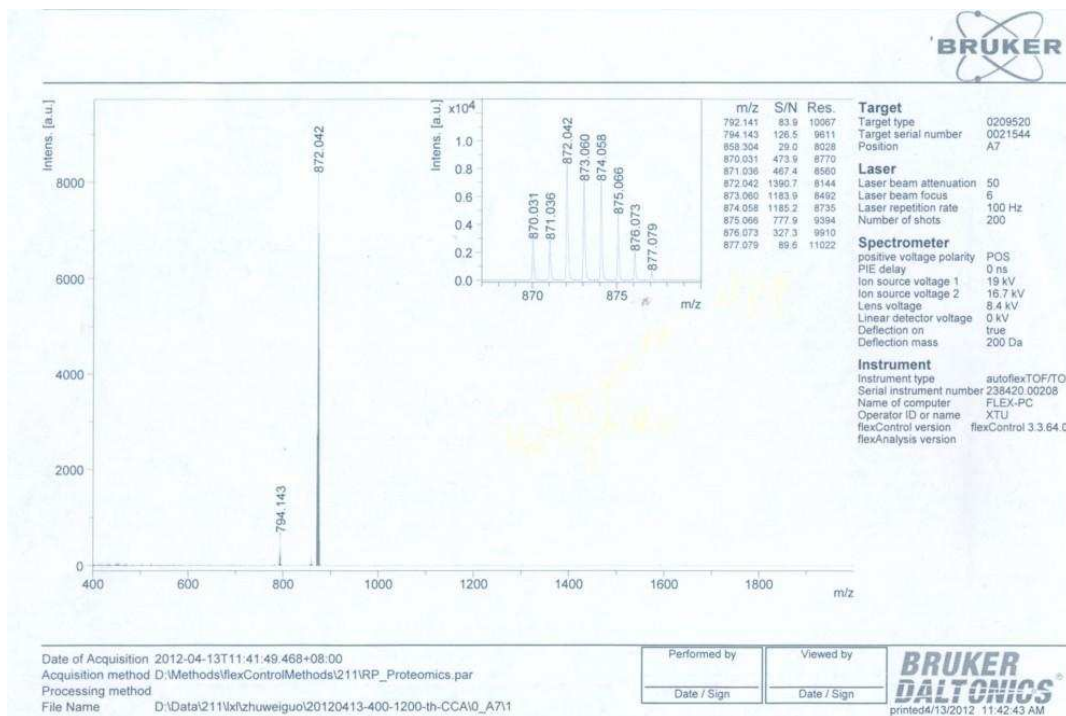


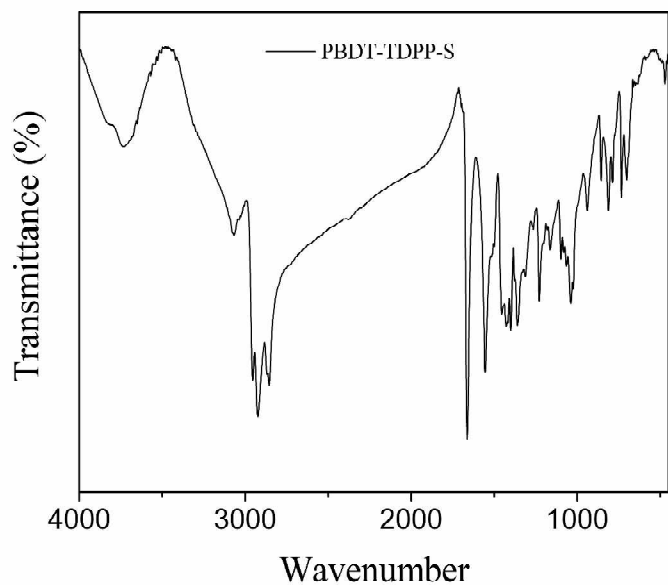
(b)

**Figure S8.** Tapping-mode AFM images of the PBDT-TDPP-S:PC<sub>71</sub>BM film (a) in unannealed condition and (b) in annealed condition at 120 °C on glass/ITO/PEDOT:PSS substrate.

9.  $^1\text{H}$  NMR data of compound 2, **M2**, PBDT-TDPP-S, and MS data of **M2**, and the infrared spectrum of PBDT-TDPP-S







## Reference

1. Wang, M.; Hu, X. W.; Liu, P.; Li, W.; Gong, X.; Huang, F.; Cao, Yong J. Am. Chem. Soc. **2011**, 133, 9638-9641.
2. He, Z. C.; Zhong, C. M.; Huang, X.; Wong, W. -Y.; Wu, H. B.; Chen, L. X.; Cao, Y. Adv. Mater. **2011**, 23, 4636-4643.